ACS Macro Letters

Letter

pubs.acs.org/macroletters

Conductivity Scaling Relationships for Nanostructured Block Copolymer/Ionic Liquid Membranes

Megan L. Hoarfrost[†,‡] and Rachel A. Segalman*[,†,§]

[†]Department of Chemical and Biomolecular Engineering, University of California, Berkeley, Berkeley, California 94720, United States

[‡]Energy and Environmental Technologies and [§]Materials Sciences Divisions, Lawrence Berkeley National Laboratory, Berkeley, California 94720, United States

Supporting Information

ABSTRACT: To optimize the properties of membranes composed of mixtures of block copolymers with ionic liquids, it is essential to understand universal scaling relationships between composition, structure, temperature, and ionic conductivity. In this work, we demonstrate the universality of relationships developed to describe the temperature and concentration dependence of ionic conductivity in such membranes by comparing the conductivity behavior of mixtures of ionic liquid with two block copolymer chemistries. The conductivities of all the mixtures are described by a single expression, which combines percolation theory with the Vogel−Tamman−Fulcher (VTF) equation. Percolation theory describes the power law dependence of conductivity on the overall volume fraction of ionic liquid, while the VTF equation takes into account the effect of the glass transition temperature of the conducting phase on the temperature dependence. The dominance of the overall volume fraction of ionic liquid in determining conductivity indicates that there is incredible flexibility in designing highly conductive block copolymer/ionic liquid membranes.

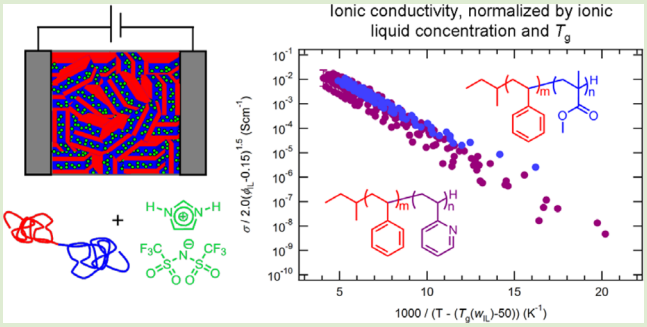

Ionic liquids, which are salts with low melting temperatures, have unique properties including low vapor pressure, high thermal, chemical, and electrochemical stability, and high ionic conductivity.[1] This exceptional combination of properties makes them outstanding candidates for ion-conducting media in a variety of electrochemical applications.[2] Selectively incorporating an ionic liquid into one block copolymer microphase allows for tunable mechanical properties and the confinement of ionic liquid to nanoscopic conducting channels.[3−12]

Understanding the relationship between composition, structure, temperature, and ionic conductivity in the resulting block copolymer/ionic liquid membranes is essential for optimizing their properties. In contrast to dilute electrolyte solutions, where ionic conductivity, σ, is simply proportional to the number of ions and the diffusion coefficients of the ionic moieties (Nernst−Einstein equation), σ scales nonlinearly with ion concentration in concentrated block copolymer/ionic liquid mixtures.[3,5,10] This is due to the combined effects of the tortuosity of the charge transport pathways, the need to be above a concentration threshold to form a percolated ionic liquid network, and the dependence of the glass transition temperature, T_g, of the conducting phase on ionic liquid concentration. Currently, there are no widely accepted scaling relationships that describe this complex behavior.

Recently, we showed that the ionic conductivity of mixtures of poly(styrene-*b*-2-vinyl pyridine) (PS-*b*-P2VP) with ionic liquids selective for the P2VP microphase can be described by the expression[3]

$$\sigma = \sigma_0(\phi_{IL} - 0.15)^{1.5} \times \exp\left\{\frac{-B}{R[T - (T_g(w_{IL}) - 50)]}\right\} \quad (1)$$

The influence of T_g on conductivity is encompassed in the second term in eq 1, which describes the temperature dependence. This term comes from the Vogel−Tamman−Fulcher (VTF) equation,[13−16]

$$\sigma = A \exp\left(\frac{-B}{R(T - T_0)}\right) \quad (2)$$

where A is a fitting parameter that contains the concentration dependence of σ, T_0 is the Vogel temperature, and B is analogous to the activation energy for ion transport in the Arrhenius equation. Like many other polymer systems, a good choice for the value of T_0 for all of the PS-*b*-P2VP mixtures was found to be about 50 K below the T_g of the P2VP/ionic liquid phase, where the T_g is a function of the weight fraction of ionic liquid exclusively in the P2VP microphase, w_{IL}. The value of B

Received: May 16, 2012
Accepted: July 6, 2012
Published: July 12, 2012

   dx.doi.org/10.1021/mz300241g | *ACS Macro Lett.* 2012, 1, 937−943

was found to be unique for each polymer/ionic liquid pair. The concentration dependence of conductivity, contained in the fitting parameter A, was found to depend on the overall volume fraction of ionic liquid, ϕ_{IL}, according to percolation theory,[17,18]

$$A = \sigma_0(\phi_{IL} - \phi_0)^n \quad (3)$$

where σ_0 is determined by the ionic conductivity of the neat ionic liquid and ϕ_0 is the percolation threshold volume fraction of ionic liquid. For PS-*b*-P2VP/ionic liquid mixtures, ϕ_0 was found to be close to the theoretical value[19] of 0.15 for an ideal, 3-D, continuous system. The power law exponent, n, is a constant that includes the effect of tortuosity, depends only on the spatial dimensions, and is 1.5 for a 3-D system. The value of n = 1.5 was found to apply to any membrane morphology for which the grains are isotropically oriented in three dimensions, including lamellar membranes, even though local transport (i.e., within a lamellar sheet) is only two-dimensional. While T_0, B, and σ_0 clearly depend on the choice of polymer and/or ionic liquid, ϕ_0 and n are geometrical parameters and are expected to be constant for different polymer/ionic liquid systems. Combining eqs 2 and 3 leads to eq 1. Equation 1 was shown to adequately describe the conductivity of PS-*b*-P2VP/ionic liquid mixtures demonstrating a wide variety of isotropically oriented morphologies having conducting phase continuity.

In this work, we compare the conductivity behavior of mixtures of ionic liquid with two block copolymer chemistries to demonstrate the universality of the scaling relationships encompassed in eq 1. The two block copolymers that were studied are PS-*b*-P2VP and poly(styrene-*b*-methyl methacrylate) (PS-*b*-PMMA). These copolymers as well as P2VP and PMMA homopolymers were combined with the ionic liquid imidazolium bis(trifluoromethylsulfonyl)imide ([Im][TFSI]), which is known to be selective for the P2VP phase in PS-*b*-P2VP and was anticipated to be selective for PMMA in PS-*b*-PMMA, because this selectivity has been previously demonstrated for other imidazolium-based ionic liquids.[10] The ionic liquid-selective component of the block copolymer was varied between the two block copolymers since the properties of the ionic liquid-containing microphase are expected to have the largest impact on ion transport. P2VP and PMMA were selected as the ionic liquid-selective polymers because their properties, for instance, their dielectric strength, pK_a, and segregation strength with PS are quite different.[20−22] The molecular weights and PS volume fractions of all polymers used in the conductivity study are listed in Table 1.

Small-angle X-ray scattering (SAXS) profiles for the PS-*b*-PMMA mixtures used in the conductivity study are shown in Figure 1a. The mixtures all demonstrate morphologies with conducting phase continuity, including lamellae (LAM), hexagonally packed PS cylinders (C_{PS}), and disordered PS micelles (DM). The mixtures containing PS-*b*-PMMA (f_{PS} = 0.78 and f_{PS} = 0.56) with ϕ_{IL} = 0.22 clearly exhibit LAM and C_{PS} morphologies, respectively, assigned based on the locations of the higher order scattering peaks. The scattering peaks for PS-*b*-PMMA (f_{PS} = 0.56) with ϕ_{IL} = 0.35 and 0.55 are very broad, suggesting PS micellar structures lacking significant long-range order (DM). DM morphologies have been observed previously for mixtures of block copolymers with ionic liquids in a similar ionic liquid concentration range.[4,6,7] The self-assembly of PS-*b*-P2VP/[Im][TFSI] mixtures was discussed in detail in a previous publication.[7] The morphologies of the mixtures used in this study include LAM, C_{PS}, and DM, as well as body-centered cubic (BCC) PS spheres ($S_{PS,BCC}$) and face-centered cubic (FCC) PS spheres ($S_{PS,FCC}$).[3] SAXS profiles for selected PS-*b*-P2VP mixtures have been reproduced in Figure 1b to facilitate comparison to those of the PS-*b*-PMMA mixtures. Some of the mixtures exhibit coexistence of two different morphologies or two different domain spacings of the same nanostructure. For example, the distinct shoulders on the scattering peaks for PS-*b*-P2VP (f_{PS} = 0.62) with ϕ_{IL} = 0.18 in Figure 1b suggest coexistence of two different lamellar domain spacings. Phase coexistence is characteristic of mixtures of block copolymers with a third component, and has been observed previously for mixtures of block copolymers with ionic liquids or salts.[4−6,23,24]

The selectivity of [Im][TFSI] for one microphase in PS-*b*-PMMA is confirmed by the shift of the primary SAXS peak of lamellar mixtures to lower q upon ionic liquid addition coupled with the decrease in T_g of only one phase (Figure 2). The T_g of the ionic liquid-containing microphase collapses as a function of w_{IL}, assuming complete segregation of the ionic liquid to the PMMA phase, confirming that [Im][TFSI] is selective for PMMA specifically. The order of lyotropic phase transitions upon ionic liquid addition also reflects this selectivity: for instance, swelling of the PMMA microphase leads to the lyotropic phase transition from hexagonally packed PMMA cylinders (C_{PMMA}) in pure PS-*b*-PMMA (f_{PS} = 0.78; characterized by a higher order peak at $\sqrt{3}q^*$) to LAM in a mixture with ϕ_{IL} = 0.07 (characterized by higher order peaks at integer multiples of q^*).

The bulk ionic conductivities of about 400 μm thick membranes were measured using four-point probe in-plane AC impedance spectroscopy. Like the PS-*b*-P2VP/ionic liquid mixtures,[3] the conductivity of PS-*b*-PMMA/[Im][TFSI] mixtures depends on the overall ion concentration in the mixture as well as how far the temperature is above the T_g of the conducting phase. This is demonstrated in Figure 3 for two sets of mixtures, one having fixed w_{IL} and various f_{PS} (and, thus, various overall charge carrier concentrations, ϕ_{IL}), and the other having fixed f_{PS} and various w_{IL} (thus, various ϕ_{IL}). The conductivity of the first set of mixtures decreases with increasing f_{PS} due to the corresponding decrease in the overall charge carrier concentration (Figure 3a). The overall conductivity scales nonlinearly with ϕ_{IL}, as expected according to eq 1. They have similar temperature dependence because the T_g of the conducting phase is a function of w_{IL}, which is fixed. The conductivity of the second set increases with increasing w_{IL} due to the increase in charge carrier concentration, and the temperature dependence becomes less steep with increasing w_{IL} because the T_g decreases.

The PS-*b*-PMMA/[Im][TFSI] conductivity data, including data for PMMA homopolymer mixtures, collapse well according to eq 1 as evident in Figure 4. This indicates that

Table 1. Degree of Polymerization, Volume Fraction, and PDI of Polymers Studied

PMMA and PS-*b*-PMMA				P2VP and PS-*b*-P2VP			
M_n (kg/mol)	N_{PMMA}	f_{PS}	PDI	M_n (kg/mol)	N_{P2VP}	f_{PS}	PDI
8.2	81	0.00	1.09	12.4	118	0.00	1.07
19.1	85	0.56	1.07	15.2	102	0.29	1.07
34.6	92	0.78	1.13	20.8	115	0.42	1.02
				29.8	108	0.62	1.10
				39.3	101	0.72	1.04

dx.doi.org/10.1021/mz300241g | ACS Macro Lett. 2012, 1, 937−943

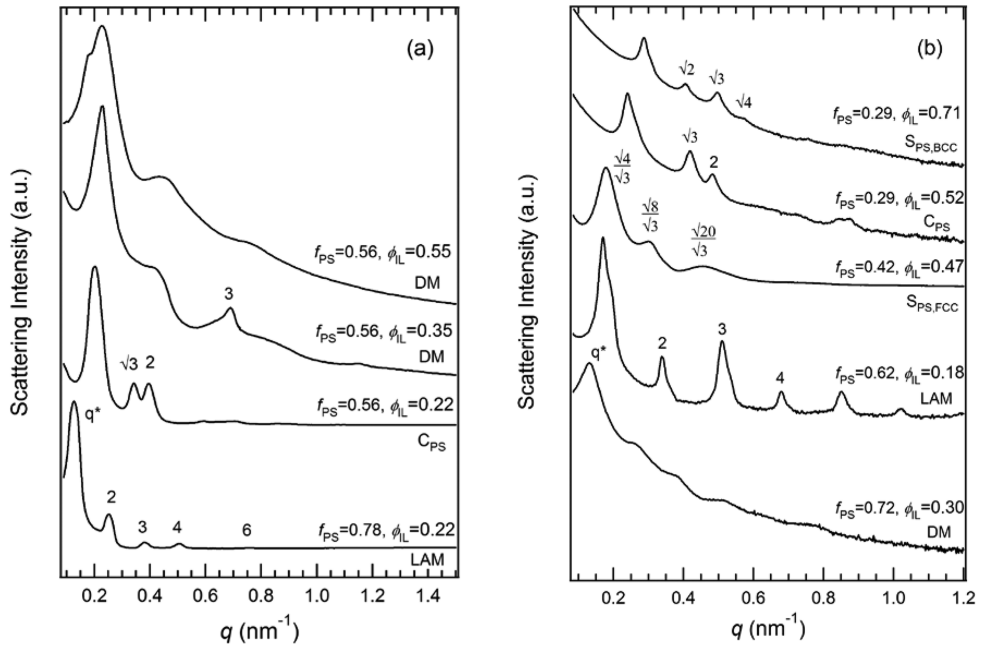

Figure 1. SAXS profiles of (a) PS-*b*-PMMA/[Im][TFSI] mixtures studied as well as (b) representative PS-*b*-P2VP/[Im][TFSI] mixtures. The PS volume fraction in the block copolymer, f_{PS}, the overall volume fraction ionic liquid in the mixture, as well as the assigned morphology of each mixture is indicated next to the corresponding scattering profile. SAXS profiles of the neat PS-*b*-PMMA block copolymers are shown in Figure S1 in Supporting Information.

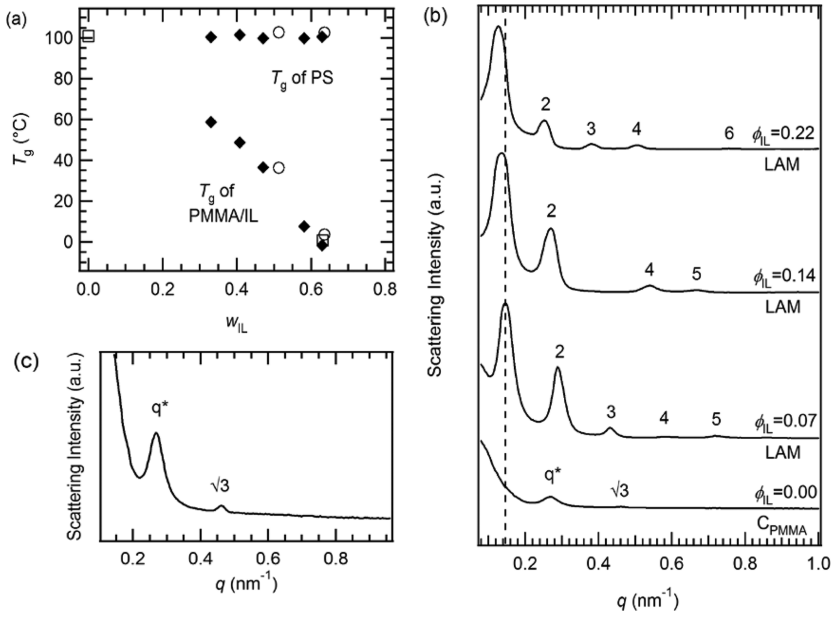

Figure 2. (a) T_g of the PS and PMMA/[Im][TFSI] phases as a function of w_{IL} for mixtures of [Im][TFSI] with PMMA (open squares), PS-*b*-PMMA (f_{PS} = 0.56; solid diamonds), and PS-*b*-PMMA (f_{PS} = 0.78; open circles). The T_g of the ionic liquid-containing microphase decreases upon ionic liquid addition, while the T_g of the PS phase remains close to 100 °C. The T_g values were determined using differential scanning calorimetry (DSC), and DSC curves are provided in Figure S2 in the Supporting Information. (b) SAXS profiles of PS-*b*-PMMA (f_{PS} = 0.78)/[Im][TFSI] mixtures, demonstrating the selectivity of [Im][TFSI] for PMMA. The overall ionic liquid volume fraction in the mixture and the assigned morphology of each mixture is indicated next to the corresponding scattering profile. (c) Blown up view of the scattering profile of pure PS-*b*-PMMA (f_{PS} = 0.78).

the form of eq 1, which accounts for total ion concentration and tortuosity of the conducting pathways separately from the plasticization effect of the ionic liquid, is universal in its ability to capture the conductivity behavior of block copolymer/ionic liquid membranes.

The slope of the PS-*b*-PMMA/[Im][TFSI] data in Figure 4 is slightly lower than that of the PS-*b*-P2VP/[Im][TFSI] data. This reflects the value of B in eq 1, which quantifies the T_g-normalized temperature dependence of conductivity, and is specific to the polymer/ionic liquid pair. We previously showed that B = 8.1 ± 1.2 kJ/mol for PS-*b*-P2VP/[Im][TFSI] mixtures.[3] VTF fits (shown in Figure 3) reveal that B = 7.3 ± 0.6 kJ/mol for PS-*b*-PMMA/[Im][TFSI]. This is quite similar, but slightly lower than B for the PS-*b*-P2VP mixtures.

dx.doi.org/10.1021/mz300241g | *ACS Macro Lett.* 2012, 1, 937−943

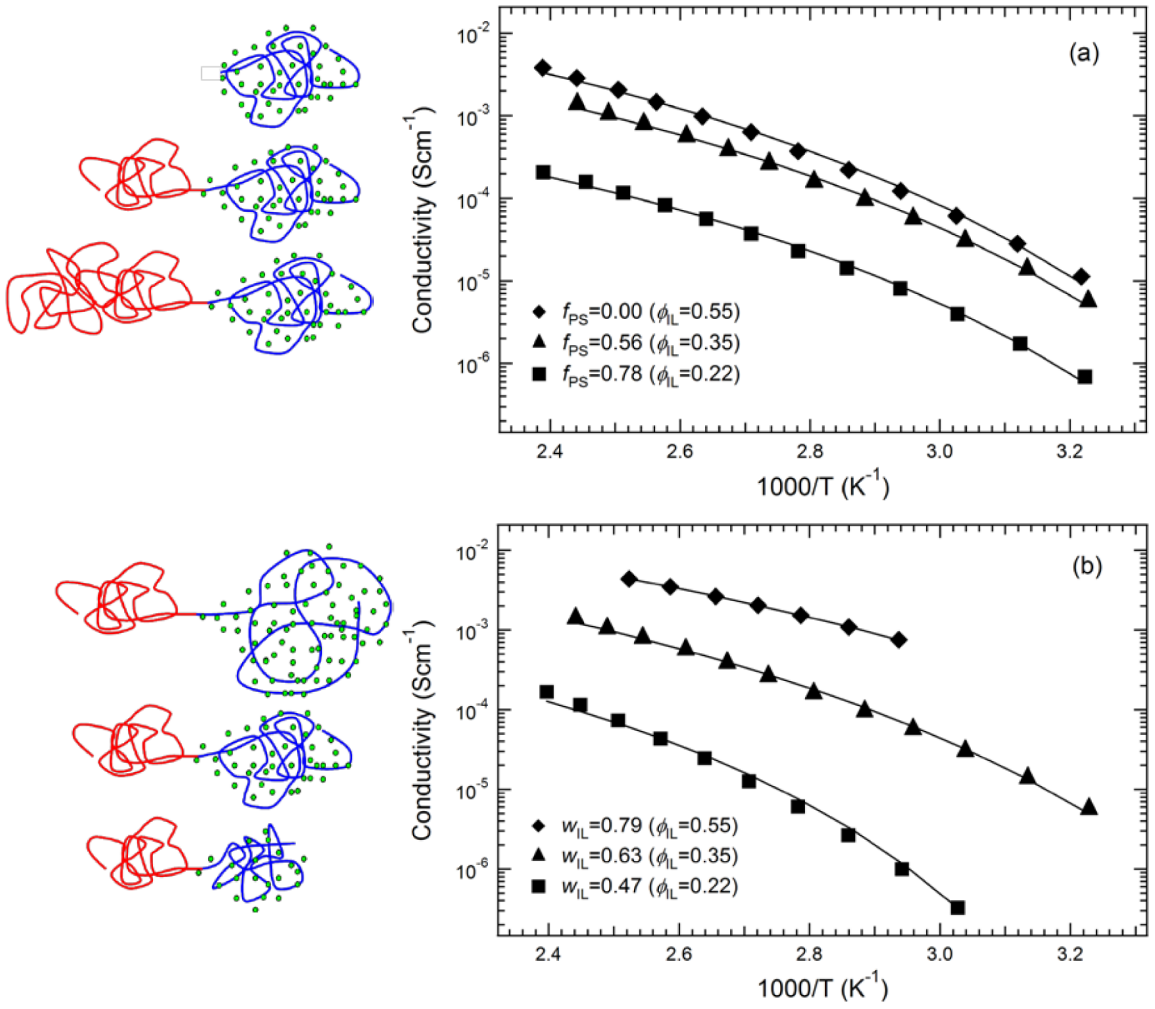

Figure 3. Ionic conductivity as a function of temperature for PS-*b*-PMMA/ [Im][TFSI] mixtures having (a) fixed w_{IL} = 0.63 and various f_{PS} and (b) fixed f_{PS} = 0.56 and various w_{IL}. Solid curves are VTF fits. Red depicts PS regions, blue depicts PMMA regions, and green depicts [Im][TFSI] in the cartoons.

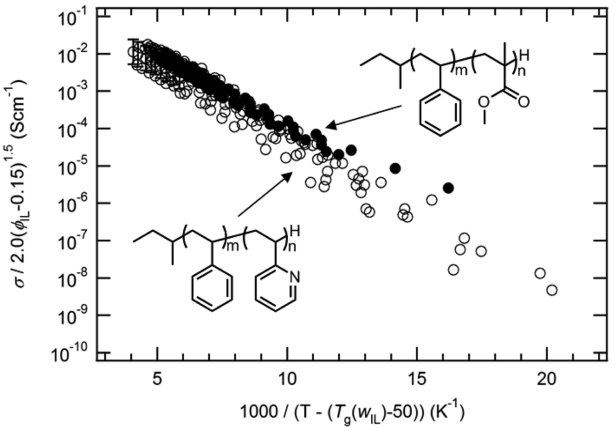

Figure 4. Conductivity of PS-*b*-PMMA/[Im][TFSI] mixtures (solid symbols) and PS-*b*-P2VP/[Im][TFSI] mixtures (open symbols), including homopolymer mixtures, plotted according to eq 1. σ_0 = 2.0 was calculated previously from the conductivity of neat [Im][TFSI].[3] For graphical clarity, the error bars are shown only for one sample. They represent a reasonable estimate based on the accuracy of AC Impedance measurements (±1/3 order of magnitude) and can be extended to all data points.

The data for both types of mixtures begin to collapse with each other at the highest experimental temperatures (lowest values of the normalized *x*-coordinate), which is the regime in which the concentration dependence described by percolation theory dominates over the temperature dependence. Figure 5

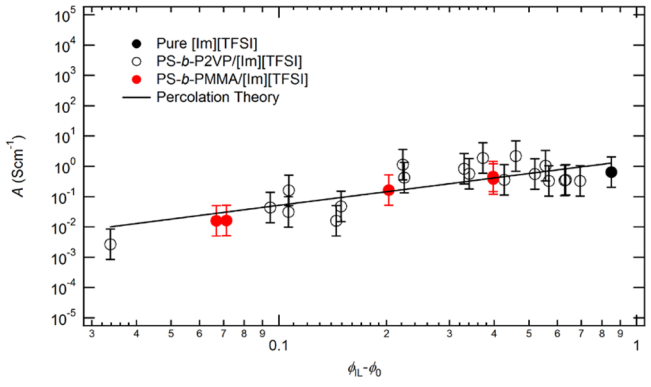

Figure 5. *A* as a function of $\phi_{IL} - \phi_0$ for PS-*b*-PMMA/[Im][TFSI] mixtures, compared to *A* for PS-*b*-P2VP/[Im][TFSI] mixtures and the percolation theory (eq 3), fit to PS-*b*-P2VP/[Im][TFSI] data. ϕ_0 is the percolation threshold volume fraction, equal to 0.15.

dx.doi.org/10.1021/mz300241g | *ACS Macro Lett.* 2012, 1, 937−943

shows this directly by comparing the fitted values of the prefactor A from VTF fits, which contains the concentration dependence of conductivity. The data for both mixtures are found to be described well by the same percolation curve fit (eq 3), as expected.

The conductivity of P2VP and PMMA homopolymer mixtures is described equally well by percolation theory as the conductivity of nanostructured block copolymer mixtures; the conductivity of each type of mixture drops off rapidly near the percolation threshold volume fraction of ionic liquid, $\phi_0 = 0.15$. This indicates that the percolation threshold is based on percolation of ionic liquid molecules either within block copolymer nanodomains or across homopolymer membranes, rather than percolation of conducting block copolymer nanodomains themselves.

The ability of percolation theory to describe the conductivity of block copolymer/ionic liquid mixtures demonstrating many different morphologies as well as homopolymer/ionic liquid mixtures also indicates the dominance of ionic liquid volume fraction in determining conductivity. The morphology imparted to the membrane via block copolymer self-assembly, while being a handle for improving mechanical and other desirable properties of the membrane, has little effect on conductivity so long as the ion-conducting domains are well-connected (and confinement does not actually influence the mechanism of ion conduction in the ionic liquid[12]). Alignment of isotropic grains could increase conductivity in the direction of alignment, but these effects are modest compared to the multiple order of magnitude effect of varying ionic liquid volume fraction. For instance, aligning membranes with lamellar channels theoretically enhances conductivity in the direction of alignment by a factor of 1.5, which is consistent with experiment.[25−27] Phase contrast between conductive and nonconductive phases is also expected to influence conductivity in other systems.[28] Phase contrast is high in all of the membranes studied in this work due to the strong selectivity of the ionic liquid for one microphase and strong segregation between the microphases.

In summary, we have shown that a single expression (eq 1) adequately describes the ionic conductivity of block copolymer/ionic liquid mixtures with multiple chemistries, where the ionic liquid is soluble in one microphase. Equation 1 paints a picture of how ion conduction occurs in block copolymer/ionic liquid mixtures, and the general scaling relationships contained therein have profound implications for the design of new materials. Clearly, choosing an ionic liquid with a high neat conductivity benefits conductivity (through the parameter σ_0). The main effect of the block copolymer on ionic conductivity is its influence on the T_g of the conducting phase. The conductivity can be improved by choosing a polymer/ionic liquid pair with a low T_g compared to the desired operating temperature. Additional factors such as specific molecular interactions between the polymer and ionic liquid[3] or ion aggregation in the presence of the polymer[29−31] affect the temperature dependence of conductivity through the parameter B, but the value of B has not been shown to vary greatly between the systems studied thus far. Other than these effects, the polymer serves only as a mechanical matrix for the ionic liquid, as evidenced by the concentration dependence term being described well by percolation theory. Thus, there is enormous flexibility in designing block copolymer/ionic liquid systems for applications requiring high ionic conductivity. This is in contrast to block copolymer/salt polymer electrolytes, for instance, where the conductivity mechanism is intimately related to specific coordination between the polymer and the salt and is, thus, extremely chemistry dependent.[32] Furthermore, because conductivity scales with the overall volume fraction of ionic liquid, a nonconductive block can be incorporated into the block copolymer to impart mechanical durability or a number of other functionalities to the membrane without sacrificing conductivity. Block copolymer membranes will have the same conductivity as a homopolymer membrane at high temperature as long as the overall ionic liquid content is maintained.

EXPERIMENTAL SECTION

Polymer Synthesis and Characterization. Poly(methyl methacrylate) (PMMA) and poly(styrene-*b*-methyl methacrylate) (PS-*b*-PMMA) were synthesized via anionic polymerization, as described previously,[33] using LiCl and 1,1-diphenylethylene as described in ref 34. The molecular weight of PMMA was determined using ^{1}H NMR end-group analysis (Bruker DRX, 500 MHz). The molecular weights of the polystyrene (PS) blocks of the block copolymers were determined using gel permeation chromatography (GPC) and the total molecular weights of the block copolymers were determined using ^{1}H NMR. GPC was used to assess the polydispersities of the block copolymers, which were found to be ≤1.13. Synthesis and characterization of poly(2-vinyl pyridine) (P2VP) and poly(styrene-*b*-2-vinyl pyridine) (PS-*b*-P2VP) were described previously.[3] The total molecular weight, M_n, the degree of polymerization of the PMMA or P2VP blocks, N_{PMMA} or N_{P2VP}, the volume fraction of PS, f_{PS}, and the polydispersity index, PDI, of each polymer are given in Table 1.

Ionic Liquid Purification and Preparation. Imidazole (≥95%) and bis(trifluoromethylsulfonyl)imide (HTFSI, ≥95%) were purchased from Sigma Aldrich and purified by sublimation under vacuum. The final purity of each starting material was assessed using differential scanning calorimetry (DSC) and ^{1}H NMR. Purified imidazole and HTFSI were combined in an equimolar ratio and heated at 110 °C for 2−3 h. The composition of the resulting [Im][TFSI] ionic liquid was confirmed by comparing the measured melting temperature, T_m, and ^{1}H NMR profile to literature.[35] Because of their hygroscopic nature, the ionic liquid and its starting materials were handled in an argon atmosphere glovebox and sealed sample holders at all times.

Preparation of Polymer/Ionic Liquid Mixtures. Dichloromethane and tetrahydrofuran were degassed using three freeze, pump, thaw cycles, dried by stirring over CaH_2 overnight, then distilled into a collection flask, brought into an argon atmosphere glovebox, and stored on molecular sieves. All further sample preparation was performed within an argon atmosphere glovebox. Predetermined quantities of [Im][TFSI] and PMMA or PS-*b*-PMMA were weighed into glass vials, about 5 wt % solutions were prepared by dissolving in tetrahydrofuran (PMMA mixtures) or dichloromethane with a few drops of tetrahydrofuran (PS-*b*-PMMA mixtures), and the solutions were stirred overnight. Samples were cast one drop at a time into sample holders for differential scanning calorimetry (DSC), small-angle X-ray scattering (SAXS), and AC impedance spectroscopy. Samples were then heated in a vacuum oven at 110 °C for around 18 h to remove remaining solvent before sample holders were sealed shut. Preparation of P2VP and PS-*b*-P2VP mixtures was described previously.[3] Samples were sealed in jars containing desiccant in the glovebox for transportation to experimental apparatuses. The weight fraction of ionic liquid exclusively in the conducting phase, w_{IL}, was determined assuming complete segregation of the ionic liquid into the P2VP or PMMA phase. The overall volume fraction of ionic liquid, ϕ_{IL}, was determined assuming ideal mixing. The density of [Im][TFSI] was estimated to be 1.67 g/cm^3 from scattering length density fits of SANS intensity profiles,[8] and the densities of PS, P2VP, and PMMA were taken to be 1.05, 1.05, and 1.18, respectively.

Differential Scanning Calorimetry (DSC). DSC samples were crimped in an argon atmosphere glovebox using hermetically sealed pans and placed inside a container with desiccant for transfer to the DSC. DSC was performed on a TA Instruments DSC Q20. Indium

dx.doi.org/10.1021/mz300241g | ACS Macro Lett. 2012, 1, 937−943

and dodecane were used as calibration standards. Samples underwent three heating and cooling cycles with a scan rate of 10 °C per minute, and the measured values of T_g or T_m from the second heating scan were recorded.

Morphology Characterization. Mixture morphologies were determined using small-angle X-ray scattering (SAXS). Samples were cast in an argon atmosphere glovebox into sample cells formed by an aluminum spacer sealed onto a Kapton window on one side until about 1 mm solid samples were obtained. After heating to remove solvent, a second Kapton window was glued to seal the samples, and the samples were sealed in jars containing desiccant for transportation to the beamline. SAXS was performed on beamline 7.3.3 of the Advanced Light Source (ALS) and beamline 1−4 of the Stanford Synchrotron Radiation Lightsource (SSRL). Samples were equilibrated within the beamline at 145 °C for 30 min before data were gathered. At the ALS, the beamline was configured with an X-ray wavelength of λ = 1.240 Å and focused to a 50 × 300 μm spot. Full two-dimensional scattering patterns were collected on an ADSC CCD detector with an active area of 188 × 188 mm. The scattering patterns were radially averaged and the scattering intensity corrected with the postion chamber intensity using Nika software package.[36] At the SSRL, the beamline was configured with an X-ray wavelength λ = 1.488 Å and focused to a 0.5 mm diameter spot. A single quadrant of a two-dimensional scattering pattern was collected on a CCD detector with an active area of 25.4 × 25.4 mm. The scattering patterns were radially averaged and corrected for detector null signal, dark current, and empty cell scattering.

Ionic Conductivity Measurements. Bulk ionic conductivity was measured using four-point probe in-plane AC impedance spectroscopy. Samples were cast and hot-pressed into a homemade, airtight, poly(ether ether ketone) cell, which contained four stainless steel electrodes and was screwed shut in an argon atmosphere glovebox. The working and reference electrodes were 0.7 cm apart and 1.7 cm long, and the samples were cast to be about 400 μm thick (measured after AC impedance measurements). The samples were heated at the highest measurement temperature for 12 h before measurements were made. Impedance measurements were performed using a Gamry Reference 600 Potentiostat at descending temperatures. An alternating current signal with an amplitude of 5 mV was applied in the frequency range of 100 to 65,000 Hz. Either the nonzero x-intercept or the minimum in the Nyquist plot of the negative imaginary part of the impedance versus the real part of the impedance was taken as the sample resistance, R. The ionic conductivity, σ, was calculated as t/AR, where t and A are the thickness and area of the sample, respectively.

■ ASSOCIATED CONTENT

Supporting Information

SAXS profiles for neat PS-*b*-PMMA block copolymers, and DSC curves for PS-*b*-PMMA/[Im][TFSI] mixtures.. This material is available free of charge via the Internet at http://pubs.acs.org.

■ AUTHOR INFORMATION

Corresponding Author

*E-mail: segalman@berkeley.edu.

Notes

The authors declare no competing financial interest.

■ ACKNOWLEDGMENTS

This material is based upon work performed by the Joint Center for Artificial Photosynthesis, a DOE Energy Innovation Hub, as follows: Material preparation and investigation of mixture morphology and conductivity was supported by the Assistant Secretary for Energy Efficiency and Renewable Energy, Office of Hydrogen, Fuel Cell, and Infrastructure Technologies of the U.S. Department of Energy under Contract No. DE-AC02-05CH11231; Continued investigation of mixture conductivity and interpretation of conductivity data was supported through the Office of Science of the U.S. Department of Energy under Award Number DE-SC0004993. M.L.H. thanks support from an NSF Graduate Research Fellowship. SAXS experiments were performed at the Advanced Light Source (ALS) and the Stanford Synchrotron Radiation Laboratory (SSRL). Both are national user facilities supported by the Department of Energy, Office of Basic Energy Sciences. We gratefully acknowledge Dr. Alexander Hexemer, Dr. Cheng Wang, and Dr. Eric Schaible for experimental assistance at the ALS and Dr. John Pople for experimental assistance at the SSRL. This report was prepared as an account of work sponsored by an agency of the U.S. Government. Neither the U.S. Government nor any agency thereof, nor any of their employees, makes any warranty, express or implied, or assumes any legal liability or responsibility for the accuracy, completeness, or usefulness of any information, apparatus, product, or process disclosed, or represents that its use would not infringe privately owned rights. Reference herein to any specific commercial product, process, or service by trade name, trademark, manufacturer, or otherwise does not necessarily constitute or imply its endorsement, recommendation, or favoring by the U.S. Government or any agency thereof. The views and opinions of authors expressed herein do not necessarily state or reflect those of the United States Government or any agency thereof.

■ REFERENCES

(1) Wasserscheid, P.; Welton, T. *Ionic Liquids in Synthesis*; Wiley-VCH Verlag: Weinheim, 2003.
(2) Ohno, H. *Electrochemical Aspects of Ionic Liquids*; Wiley-Interscience: New York, 2005.
(3) Hoarfrost, M. L.; Segalman, R. A. *Macromolecules* **2011**, *44* (13), 5281−5288.
(4) Simone, P. M.; Lodge, T. P. *Macromolecules* **2008**, *41* (5), 1753−1759.
(5) Simone, P. M.; Lodge, T. P. *ACS Appl. Mater. Interfaces* **2009**, *1* (12), 2812−2820.
(6) Virgili, J. M.; Hexemer, A.; Pople, J. A.; Balsara, N. P.; Segalman, R. A. *Macromolecules* **2009**, *42* (13), 4604−4613.
(7) Virgili, J. M.; Hoarfrost, M. L.; Segalman, R. A. *Macromolecules* **2010**, *43* (12), 5417−5423.
(8) Virgili, J. M.; Nedoma, A. J.; Segalman, R. A.; Balsara, N. P. *Macromolecules* **2010**, *43* (8), 3750−3756.
(9) Kim, S. Y.; Kim, S.; Park, M. J. *Nature Commun.* **2010**, *1*, 88.
(10) Gwee, L.; Choi, J. H.; Winey, K. I.; Elabd, Y. A. *Polymer* **2010**, *51* (23), 5516−5524.
(11) Kim, S. Y.; Yoon, E.; Joo, T.; Park, M. J. *Macromolecules* **2011**, *44* (13), 5289−5298.
(12) Hoarfrost, M. L.; Tyagi, M. S.; Segalman, R. A.; Reimer, J. A. *Macromolecules* **2012**, *45* (7), 3112−3120.
(13) Fulcher, G. S. *J. Am. Ceram. Soc.* **1925**, *8* (12), 789−794.
(14) Fulcher, G. S. *J. Am. Ceram. Soc.* **1925**, *8* (6), 339−355.
(15) Tammann, G.; Hesse, W. *Z. Anorg. Allg. Chem.* **1926**, *156* (4), 245.
(16) Vogel, H. *Physik. Z.* **1921**, *22*, 645−646.
(17) Hunt, A. G.; Ewing, R. P. *Percolation Theory for Flow in Porous Media, Lecture Notes in Physics*; Springer: Berlin, 2009.
(18) Kirkpatr., S. *Rev. Mod. Phys.* **1973**, *45* (4), 574−588.
(19) Scher, H.; Zallen, R. *J. Chem. Phys.* **1970**, *53* (9), 3759−3761.
(20) *CRC Handbook of Chemistry and Physics*, 92 ed.; Taylor and Francis Group, LLC: New York, 2011−2012.
(21) Zhao, Y.; Sivaniah, E.; Hashimoto, T. *Macromolecules* **2008**, *41* (24), 9948−9951.

(22) Schulz, M. F.; Khandpur, A. K.; Bates, F. S.; Almdal, K.; Mortensen, K.; Hajduk, D. A.; Gruner, S. M. *Macromolecules* **1996**, *29* (8), 2857−2867.
(23) Young, W. S.; Brigandi, P. J.; Epps, T. H. *Macromolecules* **2008**, *41* (17), 6276−6279.
(24) Young, W. S.; Epps, T. H. *Macromolecules* **2009**, *42* (7), 2672−2678.
(25) Li, J.; Park, J. K.; Moore, R. B.; Madsen, L. A. *Nat. Mater.* **2011**, *10* (7), 507−511.
(26) Park, M. J.; Balsara, N. P. *Macromolecules* **2010**, *43* (1), 292−298.
(27) Park, J. K.; Li, J.; Divoux, G. M.; Madsen, L. A.; Moore, R. B. *Macromolecules* **2011**, *44* (14), 5701−5710.
(28) Kim, Y. S.; Pivovar, B. S. *Ann. Rev. Chem. Biomol. Eng.* **2010**, *1*, 123−148.
(29) Noda, A.; Hayamizu, K.; Watanabe, M. *J. Phys. Chem. B* **2001**, *105* (20), 4603−4610.
(30) Susan, M. A.; Kaneko, T.; Noda, A.; Watanabe, M. *J. Am. Chem. Soc.* **2005**, *127* (13), 4976−4983.
(31) Hou, J. B.; Zhang, Z. Y.; Madsen, L. A. *J. Phys. Chem. B* **2011**, *115* (16), 4576−4582.
(32) Gray, F. M., *Solid Polymer Electrolytes: Fundamentals and Technological Applications*; VCH Publishers, Inc.: New York, 1991.
(33) Yokoyama, H.; Mates, T. E.; Kramer, E. J. *Macromolecules* **2000**, *33* (5), 1888−1898.
(34) Varshney, S. K.; Hautekeer, J. P.; Fayt, R.; Jerome, R.; Teyssie, P. *Macromolecules* **1990**, *23* (10), 2618−2622.
(35) Noda, A.; Susan, A. B.; Kudo, K.; Mitsushima, S.; Hayamizu, K.; Watanabe, M. *J. Phys. Chem. B* **2003**, *107* (17), 4024−4033.
(36) Ilavsky, J. *J. Appl. Crystallogr.* **2012**, *45* (2), 324−328.